

  
**MITSUBISHI HEAVY INDUSTRIES, LTD.**  
16-5, KONAN 2-CHOME, MINATO-KU  
TOKYO, JAPAN

December 2, 2009

Document Control Desk  
U.S. Nuclear Regulatory Commission  
Washington, DC 20555-0001

Attention: Mr. Jeffery A. Ciocco

Docket No. 52-021  
MHI Ref: UAP-HF-09547

**Subject:** MHI's Responses to US-APWR DCD RAI No. 465-3382

**Reference:** 1) "Request for Additional Information No. 465-3382 Revision 1, SRP Section: 03.12 – ASME Code Class 1, 2, and 3 Piping Systems and Piping Components And Their Associated Supports," dated 10/6/2009.  
2) "MHI's Responses to US-APWR DCD RAI No. 465-3382 Revision 1," UAP-HF-09530, dated 11/18/2009.

With this letter, Mitsubishi Heavy Industries, Ltd. ("MHI") transmits to the U.S. Nuclear Regulatory Commission ("NRC") a document entitled "Responses to Request for Additional Information No. 465-3382, Revision 1."

Enclosed are the responses to 2 RAIs contained within Reference 1. This transmittal, in addition to six RAI responses previously provided in Reference 2, completes the response to this RAI.

Please contact Dr. C. Keith Paulson, Senior Technical Manager, Mitsubishi Nuclear Energy Systems, Inc. if the NRC has questions concerning any aspect of this submittal. His contact information is provided below.

Sincerely,



Yoshiaki Ogata,  
General Manager- APWR Promoting Department  
Mitsubishi Heavy Industries, LTD.

Enclosure:

1. Responses to Request for Additional Information No. 465-3382, Revision 1

CC: J. A. Ciocco  
C. K. Paulson



Contact Information

C. Keith Paulson, Senior Technical Manager  
Mitsubishi Nuclear Energy Systems, Inc.  
300 Oxford Drive, Suite 301  
Monroeville, PA 15146  
E-mail: [ck\\_paulson@mnes-us.com](mailto:ck_paulson@mnes-us.com)  
Telephone: (412) 373-6466

Docket No. 52-021  
MHI Ref: UAP-HF-09547

Enclosure 1

UAP-HF-09547  
Docket No. 52-021

Responses to Request for Additional Information No. 465-3382,  
Revision 1

December, 2009

---

---

**RESPONSE TO REQUEST FOR ADDITIONAL INFORMATION**

---

---

12/2/2009

**US-APWR Design Certification  
Mitsubishi Heavy Industries  
Docket No. 52-021**

**RAI NO.:** NO. 465-3382 REVISION 1  
**SRP SECTION:** 03.12 – ASME CODE CLASS 1, 2, AND 3 PIPING SYSTEMS AND PIPING COMPONENTS AND THEIR ASSOCIATED SUPPORTS  
**APPLICATION SECTION:** 3.12  
**DATE OF RAI ISSUE:** 10/06/2009

---

**QUESTION NO. 03.12-17:**

DCD 3.12.5.9 discussed thermal cycling in piping connected to the RCS. MHI's evaluation for thermal cycling is addressed by preventing valve leakage. The staff noted that valve-in leakage is not required for thermal cycling to occur in bottom-connected line, where thermal cycling occurs due to the cyclic penetration and retreat of the swirl flow in the branch line. The staff is requesting MHI to identify and address thermal cycling for bottom-connected lines.

In response to Question No. 03.12-10, (RAI 260-2023, MHI Ref: UAP-HF-09168, dated 4/17/2009, ML091110309) MHI stated that installation of double isolation valves decreases the possibility of leakage to the downstream of the isolation valves, which results in prevention of thermal stratification or oscillation. However, this does not ensure that leakage would not occur. Explain if any other activity could detect this low possibility leakage before causing any thermal stratification or oscillation.

---

**ANSWER:**

High temperature water flow that flows as a series of swirls is referred to as "cavity flow." This phenomenon occurs from the RCS pipe run to each stagnant branch line isolated by a valve. In addition, stratification at the surface boundary occurs between the high temperature water entering the branch pipe and the low temperature water already in the branch. When the stratified surface boundary (top of cavity flow) occurs at horizontal pipe bends and elbows, there is a possibility of significant thermal fluctuation inducing high-cycle thermal fatigue at this point (refer to Fig. 1, case B). As a result, the US-APWR pipe routing is made such that the stratified surface boundaries are not located at horizontal pipe bends and elbows along isolated branch pipes connected to the RCS.

As a prediction method, the piping route design is conducted such that the position of the stratification surface is not located at bending pipes and elbows migrating horizontally from vertical risers, based upon the evaluation models of cavity flow penetration length which is established based on test data conducted domestically in Japan. The subject research results have become publicly known at the 10th and 11th International Conference on Nuclear Engineering (refer to ICONE10-23340 and ICONE11-36214).

Furthermore, as verification of actual equipment, confirmation is made such that there is no stratification surface boundary (top of cavity flow) at pipe bends and elbows migrating horizontally from vertical risers by performing temperature measurement for actual equipment of isolated branch pipes around RCS during initial startup test.

The safety-related parts which apply double isolation valves from RCS are shown in Table 1 (downstream of RV vent line, excess letdown line, Cavity/RCS water level meter line and loop drain line are not safety-related.) If there is leakage from RCS to the downstream of these parts, the leakage can be detected by the instruments shown in Table 1.

Table 1 Detection of Leakage (for Safety-Related Part)

Part		Detection of leakage
Reactor Vessel	Direct Vessel Safety Injection Line	Leakage can be detected by temperature detector instrument downstream of in series, double check valves.
Hot Leg	Hot Leg Recirculation Line	Leakage can be detected by temperature detector instrument downstream of MOV.
	Containment Spray/Residual Heat Removal Pump Hot Leg Suction Line	Leakage can be detected by temperature detector instrument downstream of in series, double MOVs.
	Emergency Letdown Line	Leakage can be detected by temperature detector instrument downstream of in series, double MOVs.
Cold Leg	Accumulator Injection Line	Leakage can be detected by level meter or pressure gauge instrument in Accumulator.
	Residual Heat Removal Discharge Line	Downstream of in series, double check valves is normally-closed MOV. This provides triple isolation from the RCS, which is assumed to be sufficient to limit the leakage.

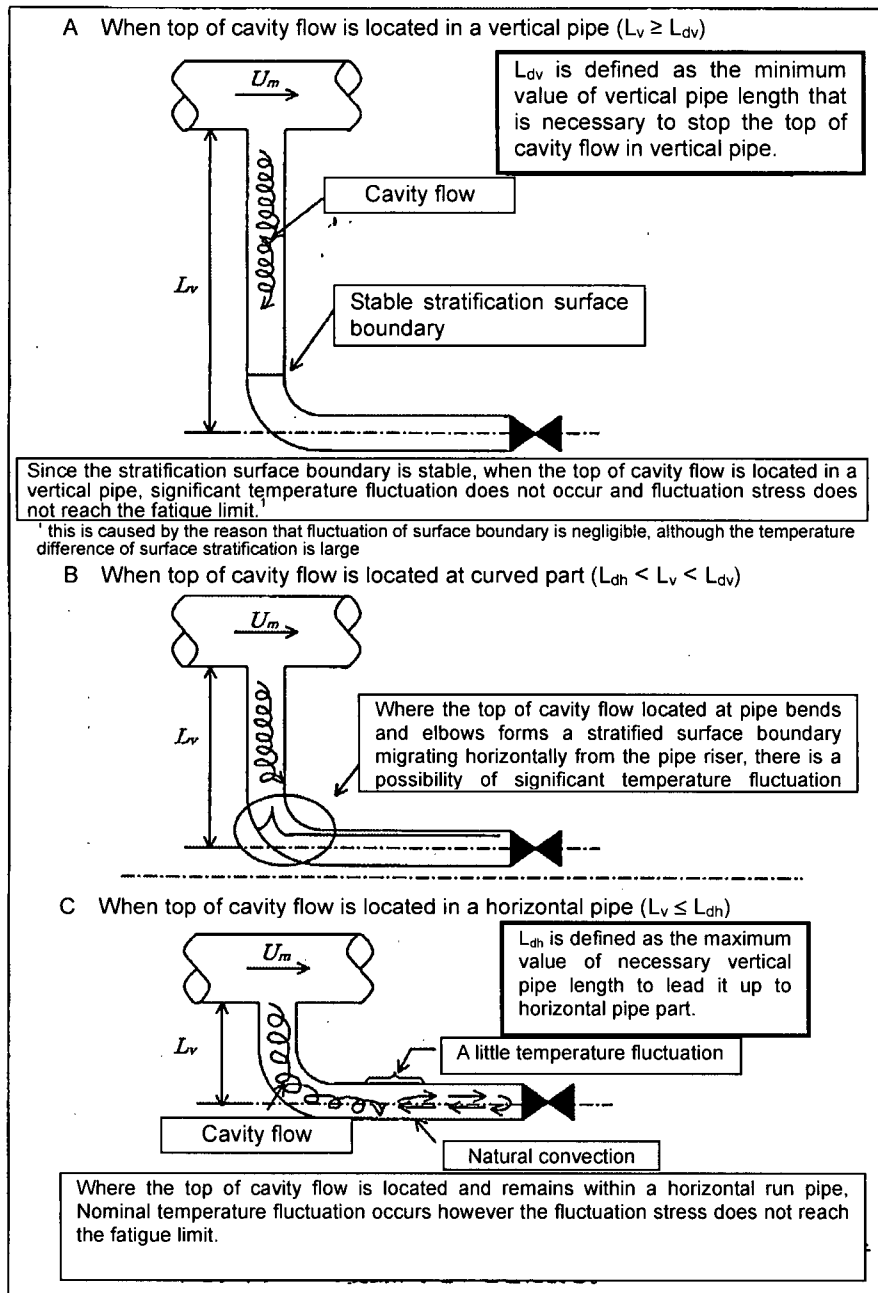


Fig.1 Briefing of Evaluation for the Structural Integrity

**Impact on DCD**

See Attachment 1 for a mark-up of DCD Tier 2, Section 3.12 changes to be incorporated.

Add the following as the last paragraph in Subsection 3.12.5.9:

“Furthermore, high temperature water that flows from the RCS pipe run into isolated branch pipes occurs as swirling water, referred to as cavity flow induced by the high temperature pipe. In addition, there is a phenomenon in which stratification occurs at the surface boundary between the high temperature water entering the branch pipe and the low temperature water already in the branch. When the stratified surface boundary (top of cavity flow) occurs at horizontal pipe bends and elbows, there is a possibility of significant thermal fluctuation inducing high cycle thermal fatigue at this point. Therefore, the piping is routed such that a stratified surface boundary does not occur at horizontal pipe bends and elbows.”

**Impact on COLA**

There is no impact on the COLA.

**Impact on PRA**

There is no impact on the PRA.

---

---

---

**RESPONSE TO REQUEST FOR ADDITIONAL INFORMATION**

---

---

12/2/2009

**US-APWR Design Certification**

**Mitsubishi Heavy Industries**

**Docket No. 52-021**

**RAI NO.:** NO. 465-3382 REVISION 1  
**SRP SECTION:** 03.12 – ASME CODE CLASS 1, 2, AND 3 PIPING SYSTEMS AND PIPING COMPONENTS AND THEIR ASSOCIATED SUPPORTS  
**APPLICATION SECTION:** 3.12  
**DATE OF RAI ISSUE:** 10/06/2009

---

**QUESTION NO. 03.12-23:**

**FOLLOW UP QUESTION TO RAI 03.12-7 (RAI No. 260-2023, Rev. 1):** In response to Question No. 03.12-7, MHI reiterated the same criteria as stated in the DCD without providing any technical justifications. MHI did not explain why the response at the branch connection point will not differ significantly when using the nearest support point spectra, nor why adding the SAM based on pipe run dynamic response to the inertial analysis of the decoupled pipe ensures conservatism.

(a) MHI stated that the response at the connection point is influenced by the input floor response spectra used for the pipe run analysis, and will not differ significantly from the floor response spectra applicable for the elevations in the near vicinity. Explain why this will not differ significantly or will not be amplified by the piping between the nearby supports and the branch connection point.

(b) Also, MHI stated that absolute addition of the solutions from the static analysis of connection movements resulting from the seismic inertia analysis of the run pipe to the solutions from the seismic inertia analysis of the decoupled branch pipe ensures conservatism. Demonstrate how this procedure ensures conservatism.

---

**ANSWER:**

MHI acknowledges that it will be difficult to prove that there is no significant amplification at the junction point on the main run by reviewing results from a floor response modal summation type of analysis. As such, MHI proposes to revise DCD Tier 2, Subsection 3.12.4.4 to reflect that if amplified response spectra at the junction point can not be developed, modeling of the branch pipe will be included in the main run analysis.

The fourth paragraph in Subsection 3.12.4.4 that starts as "If amplified response spectra ...." will be deleted. A new paragraph, which is shown below, will be added as the last paragraph in this Subsection.

If amplified response spectra at the connection point can not be developed, then modeling of the branch pipe is included in the analysis model of the run pipe. The portion of the branch pipe included in the analysis ends at either (a) the first anchor (including equipment nozzle or

containment penetration) or (b) four seismic supports in each of the three perpendicular directions. In case of option (b), the overlapping method of NUREG/CR-1980 (Reference 3.12-41) is used.

#### **Impact on DCD**

See Attachment 1 for mark-up of DCD Tier 2, Section 3.12 changes to be incorporated.

- Delete the fourth paragraph in Subsection 3.12.4.4.

~~If amplified response spectra at the connection point can not be developed, movements of the connection point from the seismic inertia analysis of the pipe run are analyzed as anchor movements and the solution is added to the seismic analysis of the decoupled branch line by absolute summation. The envelope floor response spectrum used for the seismic analysis of the decoupled branch line includes floor response spectra applicable for the connection point or the nearest restraints on the pipe run as a component response spectrum.~~

- Add the following as the last paragraph in Subsection 3.12.4.4.

If amplified response spectra at the connection point can not be developed, then the modeling of the branch pipe is included in the analysis model of the run pipe. The portion of the branch pipe included in the analysis ends at either (a) the first anchor (including equipment nozzle or containment penetration) or (b) four seismic supports in each of the three perpendicular directions. In case of option (b), the overlapping method of NUREG/CR-1980 (Reference 3.12-41) is used.

- Add the following as the last reference in Subsection 3.12.8.

3.12-41 Dynamic Analysis of Piping, Using the Structural Overlap Method. NUREG/CR-1980, U.S. Nuclear Regulatory Commission, Washington, DC, March 1981.

#### **Impact on COLA**

There is no impact on the COLA.

#### **Impact on PRA**

There is no impact on the PRA.

---

This completes MHI's responses to the NRC's questions.

where

$$K = 0.743$$

$$L = \text{Mass point spacing (ft)}$$

$$F_R = \text{Cut-off frequency (Hz)}$$

$$E = \text{Modulus of elasticity of pipe material (psi)}$$

$$I = \text{Moment of inertia of pipe cross-section (in}^4\text{)}$$

$$W = \text{Mass per unit length of piping + insulation + contents (lbm/ft)}$$

Concentrated weights of in-line components, such as valves, flanges, and instrumentation, are also modeled as lumped masses.

Torsional effects of eccentric masses are included in the analysis.

The mass contributed by the support is included in the analysis when it is greater than 10% of the total mass of the adjacent pipe span (including pipe, contents, insulation, and concentrated masses).

#### 3.12.4.3 Piping Benchmark Program

Piping benchmark problems included in NUREG/CR-1677, Vol. 1 and 2 (Reference 3.12-17) are used to validate the PIPESTRESS computer code used in piping stress analysis. In addition, three piping benchmark problems from NUREG/CR-6414 (Reference 3.12-25) are also used to validate the PIPESTRESS computer code.

#### 3.12.4.4 Decoupling Criteria

Branch lines and instrument connections may be decoupled from the analysis model of a larger run of piping provided that either the ratio of the branch pipe mean diameter to the pipe run mean diameter ( $D_b/D_r$ ) is less than or equal to 1/3, or the ratio of the moments of inertia of the two lines ( $I_b/I_r$ ) is less than or equal to 1/25.

In addition to the size limitations, the decoupled branch line must be sufficiently flexible to facilitate the thermal expansion and seismic movements of the pipe run without constraint. As such, restraints on the branch line should not be located close to the actual pipe run connection.

Seismic analysis of the decoupled branch line is performed using applicable envelope response spectra for the decoupled branch line considering the connection point as an anchor. The envelope response spectra also include amplified response spectra at the connection point to the supporting piping run as a component response spectra. The movements (displacements and rotations) of the pipe run from the thermal, SAM or pipe break analyses is applied as anchor movements with their respective load cases in the decoupled branch line analysis.

~~If amplified response spectra at the connection point can not be developed, movements of the connection point from the seismic inertia analysis of the pipe run are analyzed as anchor movements and the solution is added to the seismic analysis of the decoupled~~

~~branch line by absolute summation. The envelope floor response spectrum used for the seismic analysis of the decoupled branch line includes floor response spectra applicable for the connection point or the nearest restraints on the pipe run as a component response spectrum.~~

The pipe run seismic analysis is performed without the decoupled branch. However, the mass effect is considered when the mass of half the span of the branch pipe is greater than 10% of the mass of the pipe run span.

In the analysis of the pipe run, as well as the decoupled branch pipe, the effects of the applicable stress intensification factors and/or stress indices of the branch connection are incorporated.

If amplified response spectra at the connection point can not be developed, then the model of the branch pipe is included in the analysis model of the run pipe. The portion of the branch pipe included in the analysis ends at either (a) the first anchor (including equipment nozzle or containment penetration) or (b) four seismic supports in each of the three perpendicular directions. In case of option (b), overlapping method of USNRC NUREG/CR-1980 (Reference 3.12-41) is used.

### **3.12.5 Piping Stress Analysis Criteria**

#### **3.12.5.1 Seismic Input Envelope vs. Site-Specific Spectra**

The development of floor response spectra for the US-APWR design is described in Subsection 3.7.2.5, "Development of Floor Response Spectra".

If any piping is routed in tunnels or trenches in the yard, the COL Applicant is to generate site-specific seismic response spectra, which may be used for the design of these piping systems.

#### **3.12.5.2 Design Transients**

ASME Code, Section III, Class 1 (Reference 3.12-2) piping system and support component experience the RCS transients identified in Table 3.9-1. On the other hand, Class 1 piping experiences the specific transient caused by the flow injection or discharge through this piping. These transient are listed in Table 3.12-6.

#### **3.12.5.3 Loadings and Load Combination**

##### **3.12.5.3.1 Pressure**

The internal design pressure,  $P$ , is used in the design and analysis of ASME Code, Section III, Class 1, 2 and 3 piping (Reference 3.12-2). The wall thicknesses are determined using the formulations of NB/NC/ND-3640 and the design pressure,  $P$ . Table 3.12-1 provides the definition of terms associated with Tables 3.12-2, 3.12-3 and 3.12-4. The applicable design and maximum service level pressures are used in load combinations as identified in Tables 3.12-2 and 3.12-3.

2. For a single valve configuration, leakage can be detected by measuring the downstream temperature. Monitoring of downstream temperature is utilized to detect valve leakage. As a result of leakage detection, valve repair can be scheduled, thereby preventing fatigue failure from thermal stratification or oscillation.
3. In the case of a gate valve configuration, high-cycle fatigue could be caused by repeated leaks from the valve gland. Leaks would occur even when double isolation valves are installed in series. By permitting continuous leakage through the valve gland packing by valve disk position adjustment, valve disk expansion and contraction cycle is prevented and cyclic fatigue failure caused by thermal stratification or thermal oscillation is eliminated (Reference 3.12-27).

Furthermore, high temperature water that flows from the RCS pipe run into isolated branch pipes occurs as swirling water, referred to as cavity flow induced by the high temperature pipe. In addition, there is a phenomenon in which stratification occurs at the surface boundary between the high temperature water entering the branch pipe and the low temperature water already in the branch. When the stratified surface boundary (top of cavity flow) occurs at horizontal pipe bends and elbows, there is a possibility of significant thermal fluctuation inducing high cycle thermal fatigue at this point. Therefore, the piping is routed such that a stratified surface boundary does not occur at horizontal pipe bends and elbows.

#### **3.12.5.10 Thermal Stratification**

NRC Bulletin 79-13 (Reference 3.12-28) addresses the effect of thermal stratification that lead to the cracking of the feedwater line at D.C., Cook Nuclear Plant Unit 2.

Provisions of the thermal stratification of the feedwater nozzle are described in Subsection 5.4.2.1.2.12.

NRC Bulletin 88-11 (Reference 3.12-29) was issued after Portland General Electric Company experienced difficulties in setting whip restraint gap sizes on the pressurizer surge line at the Trojan plant.

At the horizontal portion of the pressurizer surge line, thermal stratification is expected to occur if the surge flow velocity is low, and to disappear if the velocity is high. At normal operation, a low flow-rate out-surge flow in the line connecting the pressurizer to the hot leg may occur due to a continuous spray, which could lead to a thermal stratification in the cross section of pressurizer surge line in accordance with the temperature difference between pressurizer and hot leg. When a high-flow rate out-surge flow or in-surge flow occurs during transient events, this thermal stratification disappears. The low flow-rate out-surge flow is recovered as soon as out-surge or in-surge ends, thus, reproducing the thermal stratification.

Structural integrity of the pressurizer surge line of the US-APWR plant is to be assured by performing the following activities for the first US-APWR plant.

1. Fatigue evaluation is to be performed by considering the repeated event of thermal stratification occurring in the pressurizer surge line. It will be confirmed

**3. DESIGN OF STRUCTURES,  
SYSTEMS, COMPONENTS, AND EQUIPMENT**

**US-APWR Design Control Document**

- 3.12-32 ASME Boiler and Pressure Vessel Code, Section III, Division 1, Subsection NF, 2001 Edition, The American Society Of Mechanical Engineers.
- 3.12-33 ASME Boiler and Pressure Vessel Code, Section III, Division 1 – Appendices, Nonmandatory Appendix F, 2001 Edition.
- 3.12-34 Structural Welding Code – Steel. AWS D1.1/D1.1M, 2006, American Welding Society.
- 3.12-35 Service Limits and Loading Combinations for Class 1 Linear-Type Supports. Regulatory Guide 1.124, Rev.2, U.S. Nuclear Regulatory Commission, Washington, DC, February 2007.
- 3.12-36 Service Limits and Loading Combinations for Class 1 Plate-and-Shell-Type Component Supports. Regulatory Guide 1.130, Rev.2, U.S. Nuclear Regulatory Commission, Washington, DC, March 2007.
- 3.12-37 Code Requirements for Nuclear Safety Related Concrete Structures.” ACI-349, American Concrete Institute, 2001.
- 3.12-38 Anchoring Components and Structural Supports in Concrete. Regulatory Guide 1.199, U.S. Nuclear Regulatory Commission, Washington, DC, November 2003.
- 3.12-39 IEEE Recommended Practice for Seismic Qualification of Class 1E Equipment for Nuclear Power Generating Stations, IEEE Std 344-2004, Appendix D, Institute of Electrical and Electronic Engineers Power Engineering Society, New York, New York, June 2005.
- 3.12-40 Evaluation of Potential for Pipe Breaks, Report of U.S. NRC Piping Review Committee. NUREG-1061, Volume 4, U.S. Nuclear Regulatory Commission, Washington, DC, 1984.
- 3.12-41 Dynamic Analysis of Piping, Using the Structural Overlap Method. NUREG/CR-1980, U.S. Nuclear Regulatory Commission, Washington, DC, March 1981.

**ICONE10-23340**

**STUDY ON RELATIONSHIP BETWEEN THERMAL STRATIFICATION AND CAVITY  
FLOW IN A BRANCH PIPE WITH A CLOSED END**

**Koichi TANIMOTO, Tadashi SHIRAISHI,  
Shigeki SUZUKI**

Mitsubishi Heavy Industries Ltd.,  
2-1-1 Shinhama Arai-cho,  
Takasago, Hyogo 676-8686, Japan

**Kouji SHIINA**  
Hitachi, Ltd., 7-2-1 Omika-cho,  
Hitachi, Ibaraki 319-1221, Japan

**Shoichi MORIYA**  
Central Research Institute of Electric Power  
Industry, 1646 Abiko, Chiba 270-1194, Japan

**Hiroshi HIRAYAMA**

Toshiba Corp., 8, Shinsugita-cho, Isogo-ku,  
Yokohama 235-8523, Japan

**Yasuhiko MINAMI,  
Hiromu ISAKA**

Kansai Electric Power Company,  
3-3-22 Nakanoshima, Kita-ku,  
Osaka 530-8270, Japan

**Toshihiko FUKUDA,  
Jun MIZUTANI**

Tokyo Electric Power Company,  
1-1-3 Uchisaiwai-cho, Chiyoda-  
ku, Tokyo 100-0011, Japan

**Haruki MADARAME**

The University of Tokyo, 2-22 Shirakata Shirane,  
Tokai-mura, Ibaraki 319-1106, Japan

**ABSTRACT**

There are a lot of types of branch pipes with a closed end in a nuclear power plant. At a branch pipe connected to a main pipe with a constant fluid velocity such as a main coolant pipe in a PWR, hot fluid penetrates into the branch pipe due to cavity flow. At the front of the cavity flow, there is the colder fluid by heat removal on the surface of a pipe, where the large temperature gradient takes place. It is necessary to evaluate the structural integrity of a pipe in the front of the cavity flow. First of all, the cavity flow experiment in the vertical branch pipe was carried out in order to obtain the database concerning the relationship between the cavity flow and estimated dominant factors. The visualized test by using acrylic pipe was performed for the branch diameter, the velocity in a main coolant pipe, which led the physical model to evaluate the characteristics of the cavity flow. However, the visualized test condition is in the atmosphere and in the temperature range from 20 to 60 degrees C. There is the difference between the properties of the visualized test and those of the actual plant. The decreasing trend of the cavity flow depends on the kinematic viscosity, and the effect of the thermal stratification on the cavity flow depends on the ratio of fluid density to temperature. To study the property effect, we performed a test in the same temperature as in the actual plant itself. In addition, in the visualized test, the effect of the piping layout on the cavity flow has been examined.

The cavity flow penetration length increases as the velocity in the main loop increases. The cavity flow penetration length is independent of the ratio of the branch pipe diameter to the main pipe diameter up to about 0.5. From the result of the same test as the actual plant condition, at approximately 200 degrees C, the fluid viscosity effect is dominant in the cavity flow penetration, and the fluid density effect is dominant at approximately 300 degrees C. The characteristics of cavity flow in a branch pipe were discussed in detail here.

**NOMENCLATURES**

D : Diameter of the main loop  
d : Diameter of the branch pipe  
L : Length of the branch pipe  
 $L_1$  : Maximum penetration length taken into account the buoyancy effect  
 $L_2$  : Minimum penetration length at the existence of the elbow or the bending pipe  
L/D : Ratio of L to D  
 $T_w$  : Temperature of the outer surface of the branch pipe  
V : Velocity of the main loop  
 $\Delta T$  : Temperature difference between the atmosphere and the main coolant  
 $\Delta T_{cr}$  : Critical temperature difference

## 1. INTRODUCTION

The cavity flow<sup>[1]</sup> occurs in the branch pipe with the closed end under the condition that there is a constant flow in the main loop which is connected with the branch pipe. According to the cavity flow, hot water is supplied into the branch pipe. On the other hand, the heat in the branch pipe is removed to the surrounding circumference, and the temperature is lower than that in the main loop<sup>[2]</sup>. The temperature difference between the branch pipe and the main loop results in the presence of the stable thermal stratification. If there is temperature fluctuation near the thermal stratification layer, the structural integrity of the pipe is discussed. In Japan, there was a leak in the excess letdown line of Mihama-2 plant due to thermal fatigue caused by the thermal stratification of the cavity flow. It is necessary to evaluate the penetration length by the cavity flow in order to prevent a pipe from damage.

Some of the authors have proposed a model for the mechanism of a cavity flow<sup>[3,4]</sup>. There are still many unknowns left, and we are studying the phenomena.

In this paper, the characteristics of the cavity flow in the branch pipe were studied in the experiments to be simulated as the same phenomenon in an actual plant.

## 2. DESIGN EVALUATION FLOW FOR THERMAL STRATIFICATION BY CAVITY FLOW

In order to keep structural integrity of the pipe, it is necessary to establish a design evaluation flow for the cavity flow phenomenon. The cavity flow is dependent on the factors as shown below.

- (a) Velocity and temperature of the main loop
- (b) Diameters of the main loop and the branch pipe
- (c) Existence of elbow or bending pipe
- (d) Horizontal length of the branch pipe

In the design flow, the concept of  $L_1$  and  $L_2$  is introduced here.  $L_1$  means maximum penetration length by cavity flow taken into account the buoyancy effect.  $L_2$  is defined as minimum penetration length at the existence of the elbow or the bending pipe. Fig.1 presents the design evaluation flow based on  $L_1$  and  $L_2$ . At the first step, the point to be judged is that the temperature difference between the atmosphere and the main coolant should be less than the critical temperature obtained by the fatigue evaluation. The second one is to check whether the vertical length from the main loop to the front of the horizontal pipe is less than  $L_1$  or not. At the last one, it is essential to design the position of the elbow or the bending pipe to keep the distance from the main loop to them less than  $L_2$ . If all of the three criteria are not satisfactory, the design of the pipe line must be rearranged or evaluated in detail.

In this study, the experiments about the cavity flow phenomenon were performed in order to establish the method to evaluate  $L_1$  and  $L_2$ .

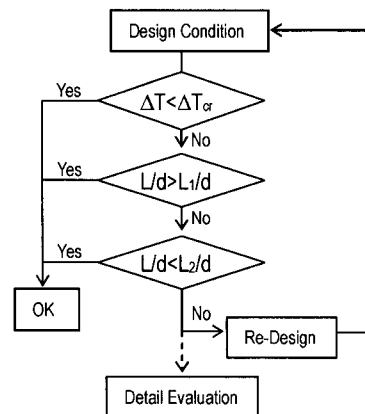


Fig.1 Design Evaluation Flow

## 3. EXPERIMENTS

The condition where the thermal stratification exists in a stable form is determined by the cavity flow and the natural circulation due to the heat removal. The natural circulation is dependent on such boundary condition as the surrounding configuration. Therefore, it is difficult to establish the method to evaluate the penetration length due to the cavity flow in an actual plant, which involves the complex loop arrangement composed by the vertical line, the horizontal line and the elbows. As the first step, the characteristics of the cavity flow were studied for the simple model. The experiments for the cavity flow were performed for the vertical branch pipe, which are the visualized test and the high temperature and pressure test. The object of the visualized test is to understand the mechanism for the stratification layer taking place by the cavity flow and the heat removal. The other's object is to investigate the effect of the property as the kinematic viscosity and the changing ratio of the fluid density on the cavity flow.

### 3.1 Visualization Tests

#### (1) Test Loop Apparatus

Fig.2 shows the apparatus of the test loop. The test loop composed of the main pipe simulated as a hot/cold leg pipe connected with a reactor vessel and cross over leg connected with a steam generator. There is an elbow above the cross over leg. Water in the tank is heated up to 60 degrees C and supplied into the loop by a pump. The test of the cavity flow in a hot/cold leg was performed without the affect of the upper stream, of which line was straight 15 D away from the junction. D means the diameter of the main loop. On the other hand, the test of the cavity flow in a cross-over leg simulated the outlet line of a steam generator. The test of the cross-over leg is estimated to be affected by the flow fluctuation due to the elbows

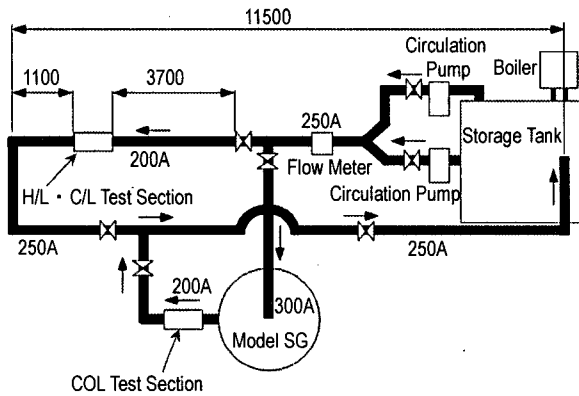


Fig.2 Visualization Tests Apparatus

(2) Test Section and Measurement Points

Fig.3 shows one of the test sections which have five types of the branch pipe diameters. Their inner diameters were manufactured so as to be consistent with the actual plant. The length of the branch pipes is 30d for the stratification layer not to be affected by the closed edge. Their materials are acrylic resin so as to be visualized. The items to be measured are the velocity in the main loop, the spiral flow velocity and temperature profile in the branch pipe, which are illustrated in Fig.4.

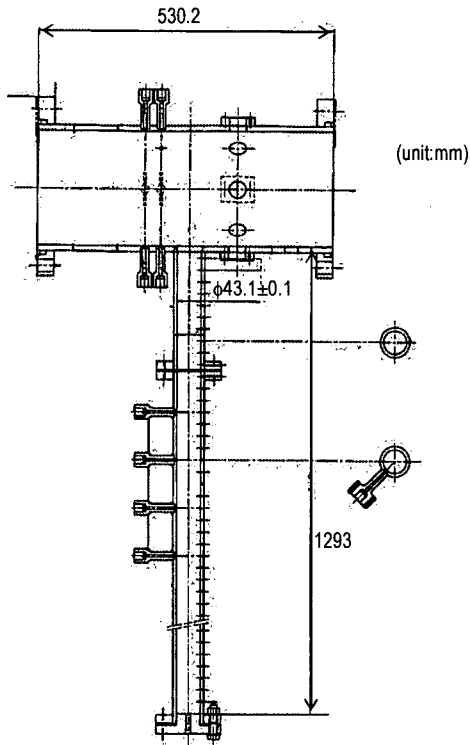


Fig.3 Sample of Test Section

The characteristics such as the temperature gradient and fluctuation of the stratification layer were measured by thermocouples. In order to establish the method to estimate the stratification layer in the vertical pipe, the vortex velocity in the branch pipe was obtained by using the hot film velocitimeter. The velocity profile in a main loop was measured by the 3 holes Pitot tube, which was applied to the discussion about the relationship between the main loop and the thermal stratification in the branch pipe.

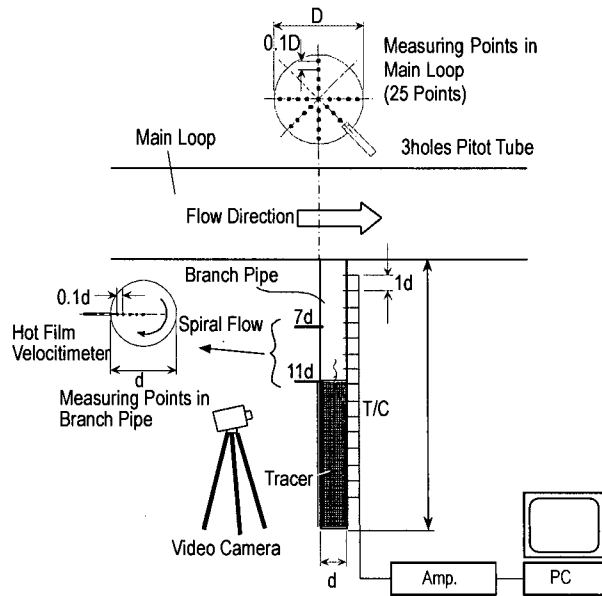


Fig.4 Concept of Measurement

(3) Test Conditions

The items as shown below are chosen from the point of view of the dominant factors to control the penetration length by the cavity flow. The summary for the test conditions is presented in Tab. 1

(a) Effect of the Velocity in the Main Loop

The velocity of the main loop is set up as 5, 11, 15 and 18m/s using the 2B branch pipe to study the effect of the main loop velocity. In addition, the effect of the branch pipe diameter on the cavity flow is investigated in the 6B branch pipe.

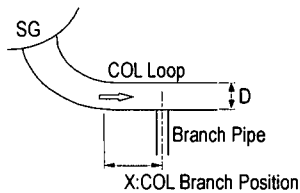
(b) Effect of the Cross Over Leg

The hydraulic phenomenon in the cross over leg from a steam generator to a pump is different from that in the hot/cold leg which has the straight pipe enough for the fully developed region. Because there are two elbows in the cross over leg, the flow pattern is estimated to be the distorted flow.

(c) Effect of the Diameter Ratio of the Branch Pipe to the Main Loop

Tab. 1 Test Conditions

Case	Main Loop			Branch Loop		
	Model	Branch Position	Velocity (m/s)	Inner Diameter (mm)	Length	
1	H/L, C/L	—	11	11.1	30d	
2				34.3		
3			5	43.1		
4						15
5						18
6			15	87.3		
7						11
8			15	128.8		
9						11
10						15
11	COL	X=0.6D	10	43.1		
12		X=1.2D				
13		X=1.8D				



It is necessary to make clear whether the penetration length by the cavity flow depends on the diameter of the branch pipe, or on the diameter ratio of the branch pipe to the main loop. The parameter experiments for the diameter of the branch pipe were carried out based on the constant ratio.

(d) Effect of the Diameter of the Branch Pipe

The penetration length by the cavity flow was investigated for the diameter of the branch pipe, that is 2B, 4B and 6B.

(e) Test Procedure

- (i) The water in the storage tank is heated up to 60 degrees C by using the boiler.
- (ii) The hot water is fed into the main loop by the circulation pump.
- (iii) The cold water (20 degrees C) is supplied from the bottom of the branch pipe on the condition that the flow in the main loop becomes stable.
- (iv) The feed of the cold water is stopped, as soon as the temperature of the connection of the branch pipe with the main loop decreases up to the temperature of the cold water.
- (v) The temperature profile in the branch pipe begins to be measured.

3.2 High Temperature and Pressure Tests

(1) Test Apparatus

Fig.5 shows the apparatus of the test loop. The water from the hot water generator which has an electric heater of 2MW power is circulated in the loop by the circulation pump. The water is pressurized by the accumulator up to a higher pressure than the saturated pressure corresponding to the fluid

temperature. There are two test sections in the main loop with a long distance enough to avoid the upper stream affect.

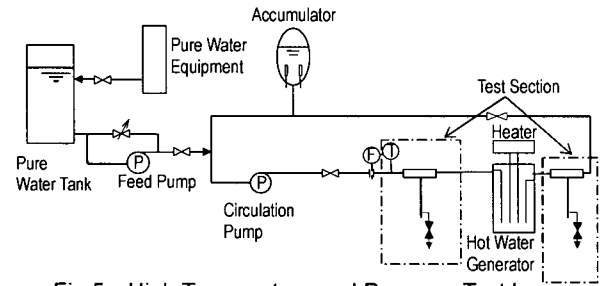


Fig.5 High Temperature and Pressure Test Loop

(2) Test Section of the Branch Pipe

Fig.6 shows a photograph of the test section with the insulator. The test section was made by the same stainless steel as the actual plant, whose specification is the outer diameter; 60.5mm, the inner diameter; 43.1mm. The length of the branch pipe is 50d straight; d means the inner diameter of the branch pipe.

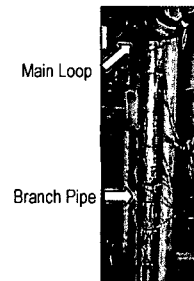


Fig.6 Apparatus of the Branch Pipe

(3) Measurement

Fig.7 shows the measuring points in order to obtain the temperature profile of the branch pipe. The temperature of the outer surface of the branch pipe was measured. In order to evaluate the stratification layer with accuracy, the thermo couples were mounted closely where the layer was estimated to appear.

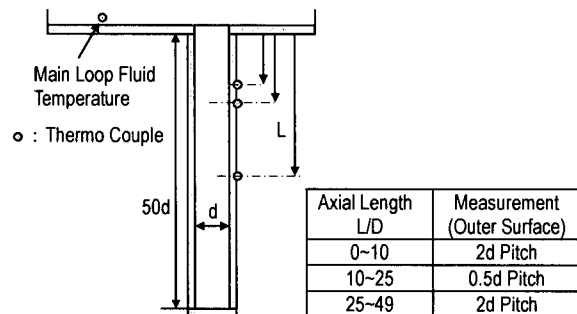


Fig.7 Measurement above the Branch Pipe

(4) Test Conditions

Tab.2 shows the summary of the test conditions in the high temperature and pressure test.

The parameter tests on the fluid temperature from 100 degrees C to 320 degrees C focus on the effect of the kinematic viscosity and the change rate of the fluid density on the penetration length by the cavity flow.

Tab. 2 Test Conditions

Run No.	Branch Pipe	Fluid Temperature [degree C]	Main Loop Velocity [m/s]
1	Vertical Line	320	15
2		290	
3		200	
4		100	

4. RESULTS

4.1 Visualization Tests

(a) Observation Results

Fig.8 shows the visualization of the cellular vortex and the spiral flow by injecting bubbles into the branch pipe. In the region of about 2d pipe length, the cellular vortex is shown to be clear. Below the clear cellular vortex, there is the unsteady flow whose direction is changing at random. After the cellular vortex is eliminated, the spiral flow penetrates into the branch pipe. The spiral flow was visualized by using the ink tracer method. On the center of the stratification layer, entrainment phenomenon occurred intermittently.

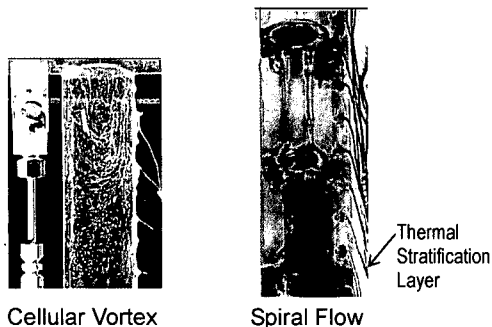


Fig.8 Visualized Results

(b) Characteristics of the Stratification Layer

Fig.9 shows the transient temperature profile of the stratification layer in the branch pipe under the condition that the velocity in the main loop is 11m/s, and the inner diameter of the branch pipe is 43.1mm. In five minutes after the start of the test, the hot fluid from the main loop penetrates deeply into the branch pipe. An hour later, the penetration rate decreases suddenly. 4 hours later, the stratification layer is stable at 18d in the branch pipe. The penetration length is defined as the most temperature gradient point along the branch pipe.

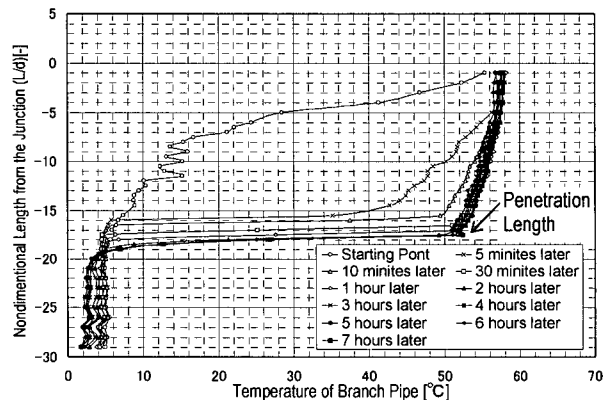


Fig.9 Temperature Profile of Thermal Stratification

(c) Effects of the Velocity of the Main Loop

Fig.10 shows the relationship between the velocity of the main loop and the penetration length of the cavity flow. The more the velocity of the main loop increases, the more the cavity flow penetrates at all types of the branch pipes.

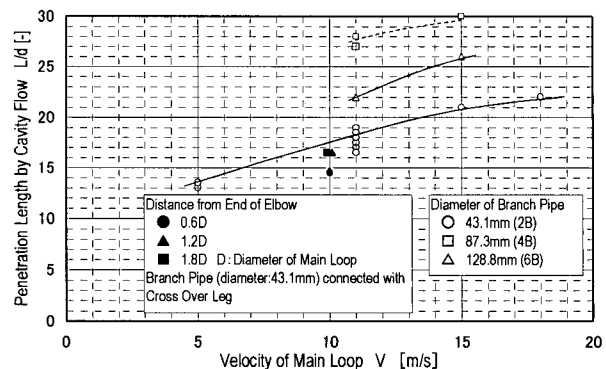


Fig.10 Relationship between Velocity of Main Loop and Penetration Length

(d) Effects of Cross Over Leg

Fig.10 as shown before, provides the relationship between the penetration length and the relative position of the branch pipe for the main loop elbow. At the 0.6D(D:the inner diameter of the main loop), the penetration length is reduced, compared with the penetration length without the elbow. However, at more than 1.2D, the penetration length is almost the same as that without the elbows. The reason is that the flow through the elbow of the main loop becomes turbulent and distorted, and that the spiral flow in the branch pipe becomes clockwise or anticlockwise at intervals from the observed results. The unstable flow in the branch pipe is considered to cause the weak penetration.

(e) Effect of the Diameter of the Branch Pipe

In Fig.11, it is clear that the penetration length becomes longer when the inner diameter of the branch pipe is larger. This tendency seems to be caused by the mechanism as mentioned below. The penetration energy induced by the cavity flow is in proportion to the interface area at the connection of the main loop with the branch pipe. Therefore, the penetration energy becomes greater as the diameter of the branch pipe becomes larger.

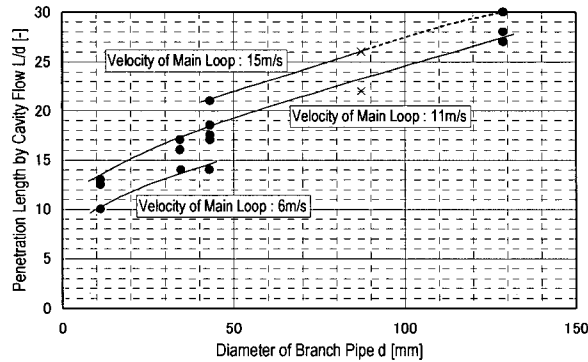


Fig. 11 Dependence of Branch Pipe Diameter on Penetration Length

(f) Effects of the Diameter Ratio of the Branch Pipe to the Main Loop

Fig.12 shows the relationship between the diameter ratio and the penetration length at 11m/s of the velocity of the main loop. Fig.12 results in that the penetration length is independent of the diameter ratio up to about 0.5.

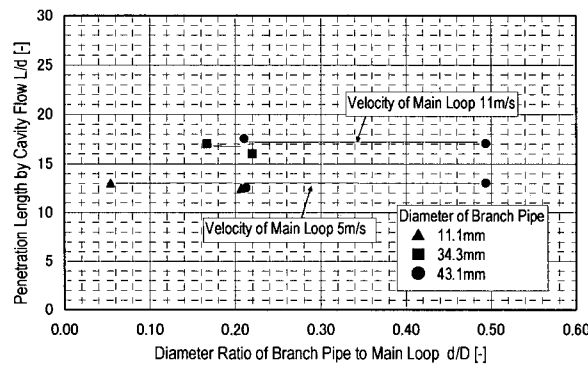


Fig. 12 Dependence of Diameter Ratio of Branch to Main Loop on Penetration Length

4.2 High Temperature and Pressure Tests

(a) Characteristics of the Cavity Flow

Fig.13 shows the transient temperature profile in the branch pipe under the condition that the velocity of the main loop is 15m/s and the fluid temperature is 320 degrees C. It

took about 40 hours for the cavity flow to become stable after the test condition was set. Fig.14 illustrates the temperature profile along the branch pipe obtained in steady state. Up to about 20d, the temperature gradient is slow and the temperature profile from this position looks as if thermal conduction in the branch pipe were dominant for the profile. From the tendency mentioned above, the penetration length is defined at the highest temperature gradient like the visualized test.

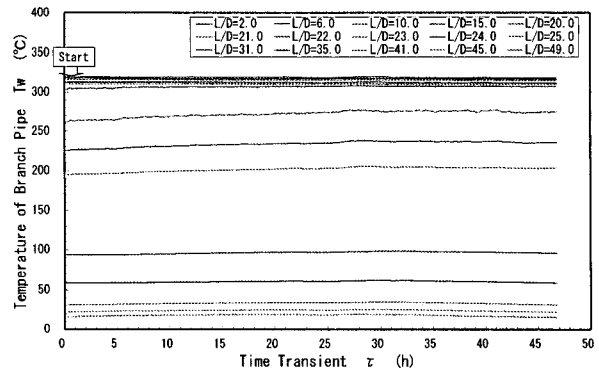


Fig. 13 Temperature Transient

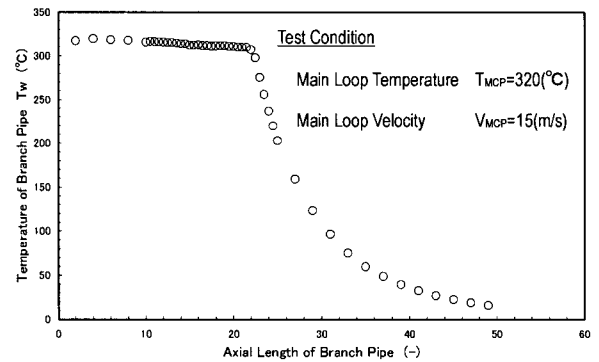


Fig. 14 Temperature Profile of Branch Pipe

(b) Dependence of the Fluid Temperature on the Penetration Length

Fig.15 shows the relationship between the penetration length and the fluid temperature of the main loop. At 100 degrees C, the penetration length is about 22.5d. If the fluid temperature of the main loop becomes high, the penetration length increases. On the contrary, when the fluid temperature is 320 degrees C, the penetration length decreases by about 2d. There seemed to be a peak at 200 degrees C for the penetration length.

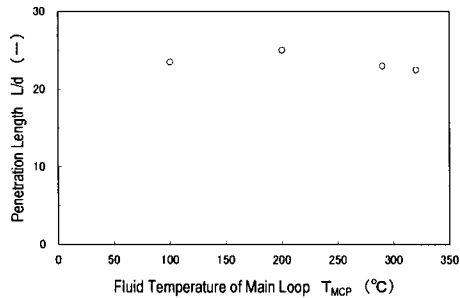


Fig. 15 Relationship between Temperature and Penetration Length

The reason to be considered is presented in Fig. 16. Fig. 16 shows the dependence of the fluid density and viscosity on temperature. The reason why the fluid density and the fluid viscosity are discussed is that the fluid density changing rate is relative to the penetration length reduction due to buoyancy force, and that the fluid viscosity is relative to the decreasing rate of the spiral flow close connected with the penetration. At first, the tendency of the penetration length up to 200 degrees C is going to be discussed. Compare the fluid of 100 degrees C with that of 200 degrees C; the changing rate in the fluid viscosity is sharper to 200 degrees C, while the changing rate in the fluid density is slower.

Therefore, the reduction of the penetration length by buoyancy force is smaller than the decreasing rate of the spiral flow by the friction loss at the inner wall, which results in the increase of the penetration length at 200 degrees C. When the fluid temperature is 320 degrees C, the fluid density changing rate is larger than the viscosity one. The reduction by the buoyancy force surpasses the decrease of the spiral flow by the shear force, which caused the reduction of the penetration length.

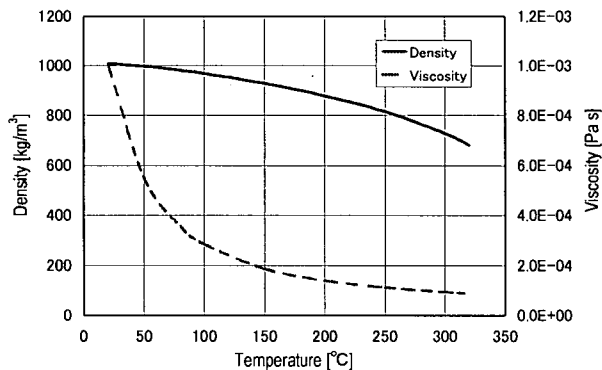


Fig. 16 Water Property (Pressure 15MPa)

## 5. CONCLUSIONS

From the results of the visualized tests and the high temperature and pressure tests, the characteristics of the penetration length by the cavity flow in the vertical branch pipe are obtained as shown below:

- The larger the velocity of the main loop becomes the longer the penetration length does.
- The penetration length is dependent not on the diameter ratio of the branch pipe to the main loop but on the diameter of the branch pipe.
- The fluid density and viscosity are dominant for the penetration length.  
The method used to estimate the penetration length in the vertical branch pipe is going to be established, based on the above conclusions,

## ACKNOWLEDGMENTS

This research is a utility-vendor joint research project on thermal stratification caused by cavity flow. Experimental results have been reviewed by a working group in the Japan Society of Mechanical Engineers with the aim of drafting a code concerning high-cycle thermal fatigue of piping systems. The authors would like to take this opportunity to express their sincere gratitude to all working group members for their important advice and support.

## REFERENCES

- Nakamori, N., et al., THERMAL STRATIFICATION IN BRANCH PIPE, NURETH6, Vol.1, pp415-424, 1993.
- Lubin, B. T. and Kim, J.H., Prediction of wall temperature distributions in long lines undergoing natural convection at high rayleigh number, Int. Chem. Eng. Symp. Ser., Vol.5, No.135, pp519-524, 1994.
- Shiraishi, T., Nabika, Y. and Suzuki, S., Experiments on a Vortex in a Circular Pipe with a Closed End, Symposium on Flow Visualization in Sapporo (SVS2000), Oct.7-8, 2000, (in Japanese).
- Shiraishi, T., Tanimoto, K. and Suzuki, S., An Engineering Model of Thermal Stratification in a Branch Pipe with a Closed End, Symposium on Flow Modeling and Turbulence Measurement (FMTM2001), Nov.4-6, 2001.

**STUDY ON RELATIONSHIP BETWEEN THERMAL  
STRATIFICATION AND CAVITY FLOW IN A BRANCH PIPE WITH A  
CLOSED END**

**(Development of Evaluation Method for Penetration Length of Cavity Flow in  
Branch Pipe Consisted of Vertical and Horizontal Pipe)**

**Yoshiyuki KONDO, Koichi TANIMOTO,**

**Tadashi SHIRAIISHI, Shigeki SUZUKI**

Mitsubishi Heavy Industries Ltd.,

2-1-1 Shinhaman Arai-cho,

Takasago, Hyogo 676-8686, Japan

**Hiroshi HIRAYAMA**

Toshiba Corp., 8, Shinsugita-cho, Isogo-ku,

Yokohama 235-8523, Japan

**Kouji SHIINA**

Hitachi, Ltd., 7-2-1 Omika-cho,

Hitachi, Ibaraki 319-1221, Japan

**Yasuhiko MINAMI,**

**Hiromu ISAKA**

Kansai Electric Power Company,

3-3-22 Nakanoshima, Kita-ku,

Osaka 530-8270, Japan

**Toshihiko FUKUDA,**

**Jun MIZUTANI**

Tokyo Electric Power Company,

1-1-3 Uchisaiwai-cho,

Chiyoda-ku, Tokyo 100-0011,

Japan

**Shoichi MORIYA**

Central Research Institute of Electric Power

Industry, 1646 Abiko, Chiba 270-1194, Japan

**Haruki MADARAME**

The University of Tokyo, 2-22 Shirakata Shirane,

Tokai-mura, Ibaraki 319-1106, Japan

Keywords: High-Cycle Thermal Fatigue, Thermal Stratification, Cavity Flow, Branch Pipe, Penetration Length

**ABSTRACT**

This paper describes the characteristics of the cavity flow which appears in a pipe with a closed end, and the development of the evaluation method of a penetration length of cavity flow. The penetration length of a cavity flow in a branch pipe with a closed end was clarified experimentally under the condition that there was a constant flow in the main loop which was connected with a branch pipe, which consist of a vertical and a horizontal pipe. The experiment was carried out for that branch pipe arrangement. In this experiment, the effect of horizontal branch pipe length and diameter, temperature, and fluid velocity in the

main loop were clarified.

The evaluation method of penetration length of cavity flow into a vertical,  $L_{sh}$ , was developed based on the experimental results. This method was consists of two model, i.e. the analysis model for cavity flow and the natural convection which appears in down stream of thermal stratification layer. It was confirmed that the method predicted penetration length of cavity flow well.

## NOMENCLATURES

$a$	: coefficient
$A$	: cross-section area
$A_i$	: cross-section area of hot and cold fluid in cavity flow
$C_p$	: specific heat
$d$	: pipe inner diameter
$D_b$	: inner diameter of branch pipe
$g$	: gravity acceleration
$h$	: enthalpy
$h_{eq}$	: equivalent heat transfer coefficient
$L$	: pipe length, penetration length
$L_{all}$	: branch pipe length
$L_0$	: length between virtual origin point and pipe junction
$L_{sh}$	: penetration length of cavity flow
$n$	: coefficient
$p$	: perimeter wet
$Q_{outH}$	: heat removal from natural convection region
$Re_d$	: Reynolds number defined by downward velocity of cavity flow
$Re_v$	: Reynolds number defined by tangential velocity of vortex
$T$	: fluid temperature in main pipe
$T_i$	: temperature at thermal stratification layer
$T_\infty$	: bulk temperature
$u$	: tangential velocity of vortex
$U$	: average velocity of fluid in main pipe
$u_o$	: velocity of vortex at pipe junction
$V$	: velocity of cavity flow
$W$	: flow rate of cavity flow
$w$	: width of boundary between hot and cold layer
$\alpha$	: velocity ratio of main pipe and inlet of branch pipe
$\delta$	: thickness of heat conduction layer
$\kappa$	: coefficient of thermal transmission
$\lambda$	: coefficient of thermal conductivity
$\lambda_{fric}$	: friction coefficient
$\nu$	: kinematic viscosity coefficient
$\rho$	: density of fluid

### Subscript

$c$	: cold layer
$f$	: fluid
$h$	: hot layer
$H$	: horizontal
$i$	: inner diameter
$o$	: outer diameter
$V$	: vertical

## 1. INTRODUCTION

The cavity flow<sup>[1]</sup> occurs in the branch pipe with the closed end under the condition that there is a constant flow in the main loop which is connected with the branch pipe. The cavity flow supplies heat, i.e. that of hot water of the main loop, into the branch pipe. On the other hand, the heat in the branch pipe is removed to the surrounding circumference, and the

temperature is lower than that in the main loop<sup>[2]</sup>. The temperature difference between the branch pipe and the main loop results in the presence of the stable thermal stratification. If there occurs temperature fluctuation near the thermal stratification layer, the structural integrity of the pipe is discussed. In Japan, there was a leak in the excess letdown line of Mihama-2 plant due to thermal fatigue caused by the thermal stratification of the cavity flow edge. It is necessary to evaluate the penetration length of the cavity flow in order to prevent a pipe from damage. Some of the authors have proposed a model for the mechanism of a cavity flow<sup>[3,4]</sup>. There are still many unknowns left, and we are studying the phenomena. In this study, the characteristics of the cavity flow in the branch pipe, which consist of a vertical and a horizontal pipe, was studied in the both visualization and high temperature and high pressure experiments. Further, the evaluation method of penetration length of cavity flow was newly developed. In this paper, the both experimental results and the evaluation method are described.

## 2. Definition of $L_{sh}$

Figure 1 shows the definition of  $L_{sh}$ , a penetration length of cavity flow in a branch pipe consisted of a vertical and a horizontal pipe connected with an elbow each other.  $L_{sh}$  is influenced by energy of a cavity flow induced by moment of fluid flowing in main pipe and heat removal from a natural convection region connecting to downward of cavity flow.

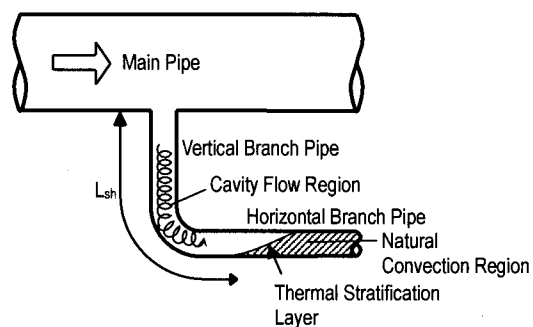
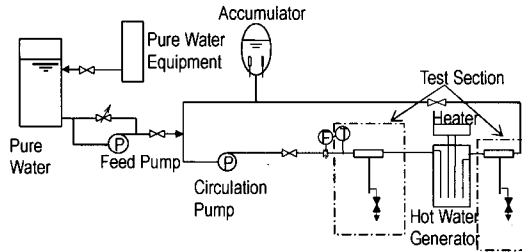


Fig.1 Definition of  $L_{sh}$

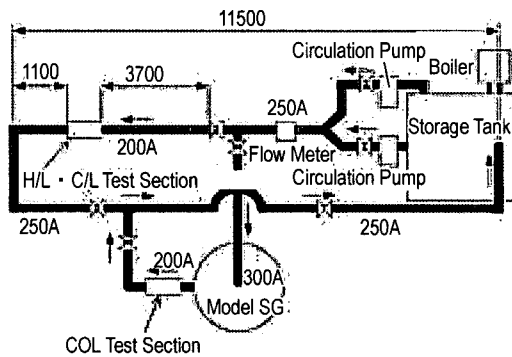
## 3. EXPERIMENT

The visualization experiment and high temperature and high pressure experiment were carried out to clarify the characteristics of cavity flow in a branch pipe. Figure 2 shows the experimental apparatus for each experiment. For the visualization experiment, the phenomenon of thermal stratification layer was clarified and for the high temperature and

high pressure experiment, the effect of the length of the horizontal pipe were clarified<sup>[5,6]</sup>. The details of those results are described following sections.



(a) Visualization Tests



(b) High Temperature and Pressure Test

Fig. 2 Schematic diagram of Experimental Set Up

#### 4. THERMAL STRATIFICATION PHENOMENON IN HORIZONTAL PIPE

##### 4.1 Visualization Experiment

Figure 3 shows the observation results of the visualization test. The cavity flow penetrate into the horizontal pipe and the thermal stratification layer appeared.

The layer fluctuate upward and backward, though, that was being steady location when it was in a vertical pipe. The cavity flow reached at the thermal stratification layer with vortex kinematic momentum and entrained cold layer. At that time, the cavity flow was attenuated by its diffusion, and it was pushed backward by the water head of the cold layer. After that, the cavity flow again increased its kinematic momentum and penetrated into the cold layer. That phenomenon described above repeated periodically. This indicates that it is not suitable to apply the evaluation method for penetration length of cavity flow into a vertical branch pipe<sup>[7]</sup>, and so another evaluation method is required. The temperature distribution along the branch pipe kept constant, and it

was contemplated that the energy from the main pipe flow and the thermal removal was balanced.

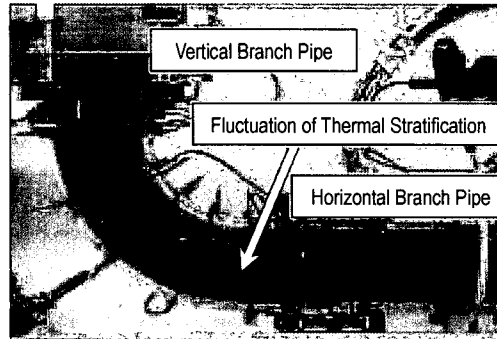


Fig.3 Visualization Experiment (Detail of Thermal Stratification)

##### 4.2 High Temperature and High Pressure Experiment

Figure 4 shows the temperature distribution along the cavity flow region for the high pressure and high temperature experiment. The decrease of temperature along the cavity flow region was larger than that for the vertical branch pipe experiment. The reason why that phenomenon caused was that the larger heat transfer from the tip of cavity flow to the natural convection region in the horizontal pipe was induced by the heat removal from the horizontal pipe.

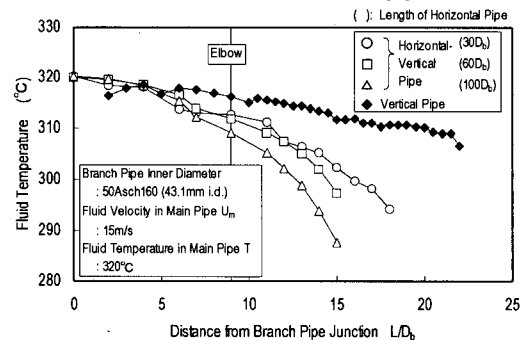


Fig.4 Distribution of Temperature along Branch Pipe

##### 4.3 Development of Evaluation Method for Cavity Flow Penetration Length

Figure 5 shows the results of the visualization experiment. The cellular vortex existed in the 4 – 6  $D_b$  section from the pipe junction and the spiral flow appeared downstream of the cellular vortex. It was confirmed in this experiment that the spiral flow existed to the thermal stratification layer. For the development of the evaluation method of the cavity flow penetration length, the spiral flow is only modeled because it is difficult to model 3-dimensional

and unsteady behaviors of the cellular vortex and the spiral flow is dominative over the cavity flow region.

## 5. EVALUATION METHOD OF $L_{sh}$

### 5.1 Outline of Evaluation Method

Penetration length of cavity flow into a branch pipe  $L_{sh}$  shown in figure 6 is calculated so that the heat input and the heat removal balances to that of correlation obtained by the experimental results. The evaluation procedure is described below.

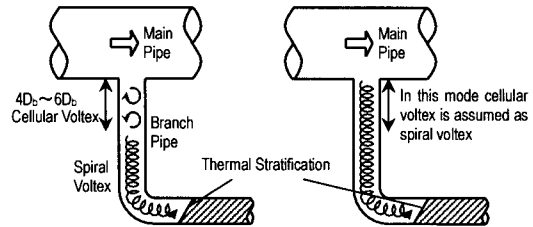


Fig.5 Model for Thermal Stratification Cavity Flow

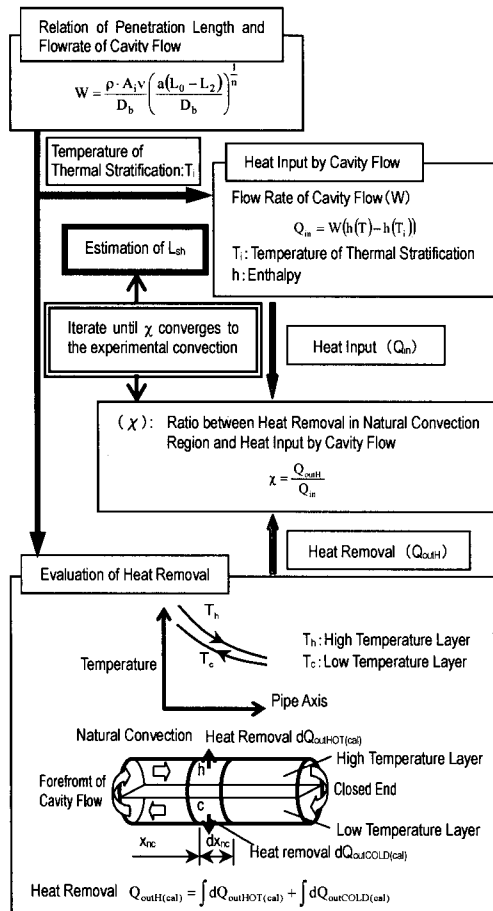


Fig.7  $L_{sh}$  evaluation procedure

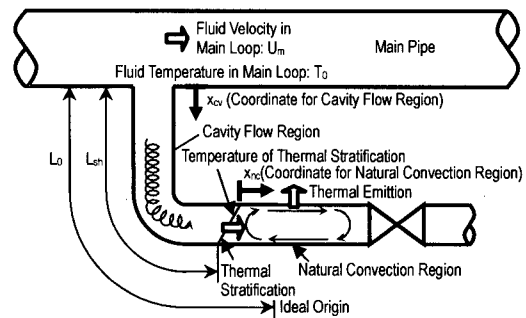


Fig.6 Outline of Analysis Model

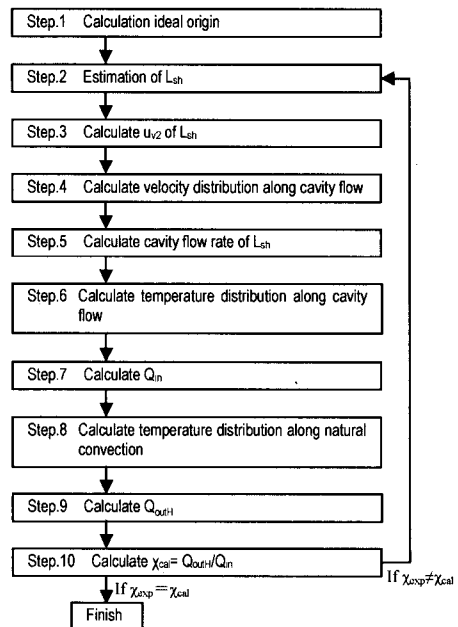


Fig.8 Procedure of Evaluation of  $L_{sh}$

Step1. Calculate virtual origin  $L_0$

$$L_0^* = \frac{L_0}{D_b} = 1.95 \text{Re}_{v0}^{0.282} \quad (1)$$

where  $\text{Re}_{v0}$  : vortex Reynolds number at inlet of branch pipe  $\left( = \frac{u_0 D_b}{\nu} \right)$ .

$u_0$  : velocity at inlet of branch pipe  
 $D_b$  : inner diameter of branch pipe  
 $\nu$  : kinematic viscosity coefficient

and,  $u_0$  is defined following equation.

$$u_0 = \alpha U$$

$\alpha$  : bifurcation ratio  $(0.2D_b + 0.0227)$   
 $U$  : fluid velocity in main pipe

Step2. assumption of  $L_{sh}$

Step3. calculate vortex velocity at top of cavity flow

$$x_{cv} = L_{sh}$$

$$\frac{L_0}{D_b} - \frac{L_{sh}}{D_b} = 1.95 \text{Re}_v^{0.282} \quad (2)$$

$$u_{v2} = \frac{\nu}{D_b} \left[ \frac{1}{1.95} \left( \frac{L_0}{D_b} - \frac{L_{sh}}{D_b} \right) \right]^{0.282}$$

Step4. calculate axial velocity distribution along cavity flow

Distance between virtual origin and stratification layer has correlation to  $\text{Re}_d$  defined by axial velocity

$$\frac{L_0}{D_b} - \frac{L(x_{cv})}{D_b} = 2.64 \text{Re}_d^{0.282} \quad (3)$$

$$u_d(x_{cv}) = \frac{\nu}{D_b} \left[ \frac{1}{2.64} \left( \frac{L_0}{D_b} - \frac{L(x_{cv})}{D_b} \right) \right]^{0.282}$$

where,  $L(x_{cv})$  is location in cavity flow

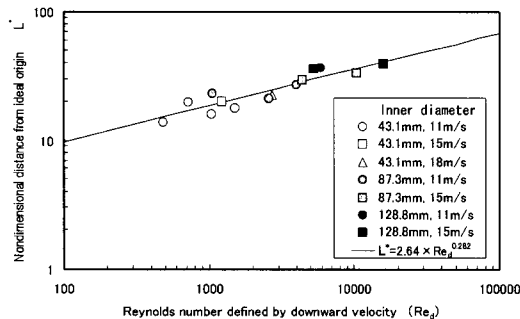


**Fig.9 Relation of Reynolds number defined by downward Velocity and Nondimensional Distance from Ideal Origin**

Step5. Calculate flow rate at forefront of cavity flow

$$\frac{L_0}{d} - \frac{L_{sh}}{d} = 2.64 \text{Re}_d^{0.282} \quad (4)$$

$$u_d = \left[ \frac{1}{2.64} \left( \frac{L_0}{D_b} - \frac{L_{sh}}{D_b} \right) \right]^{0.282}$$

$$W = \rho_f A_{cvH} u_d$$

$W$  : flow rate of cavity flow

$\rho_f$  : density of fluid

$A_{cvH}$  : cross-section area of incoming cavity flow (64% obtained by the experimental results (Fig.11))

Step6. Calculate temperature distribution along cavity flow with the equations (7) and (8) ( $x=0 \sim L_{sh}$ ), and determine temperature  $T_i$  at stratification layer

Step7. Calculate heat input  $Q_{in}$  from cavity flow region to natural convection region at stratification layer. (details are described section 5.2)

$$Q_{in} = W[h(T) - h(T_i)] \quad (5)$$

$h(T)$  : enthalpy at the temperature of  $T$

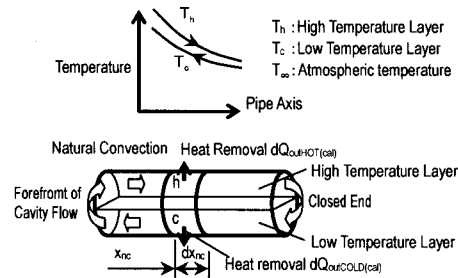
$T$  : fluid temperature in main pipe

$T_i$  : temperature at stratification layer

Step8. Calculate temperature distribution of natural convection region.(details are described section 5.2)

Step9. Calculate heat removal ( $Q_{outH}$ ) from natural convection region to atmosphere (details are described section 5.3)

$$Q_{outH(cal)} = \int dQ_{outHOT(cal)} + \int dQ_{outCOLD(cal)} \quad (6)$$



Step 10. calculate ratio of heat input from cavity flow ( $Q_{in}$ ) and heat removal from natural convection region ( $Q_{outH}$ ) ( $\chi$ ), and compare

$$\chi_{exp} \left( = \frac{Q_{outH(exp)}}{Q_{in(exp)}} \right) \quad \text{obtained}$$

$$\text{experimentally and } \chi_{cal} \left( = \frac{Q_{outH(cal)}}{Q_{in(cal)}} \right)$$

calculated. If  $\chi_{exp}$  is equal to  $\chi_{cal}$ ,  $L_{sh}$  is

determined. If  $\chi_{exp}$  is not equal to  $\chi_{cal}$ , recalculate from step 2 assuming  $L_{sh}$  again.

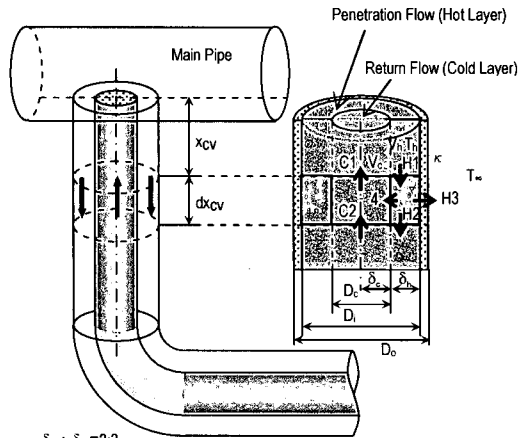
## 5.2 Calculation of Cavity Flow

### Phenomenon

In this method, cavity flow region is divided into two region as is shown in figure 11, i.e. cavity flow incoming region and returning region, and the fundamental equations 7 and 8 are formulated based on the heat balance in the infinitesimal section as following.

- (1) Inflow and outflow of heat due to fluid motion and heat conduction
- (2) Heat removal from cavity flow region to atmosphere
- (3) Heat transfer from incoming region to returning one.

The ratio of the cavity flow incoming and returning region is 2:3 in the radial direction and that is obtained experimentally (see figures 12 and 13).



$\delta_h : \delta_c = 2:3$   
(Determined from the experimental results (Fig11))

**Fig.10 Outline of Cavity Flow Model**

Incoming region

$$\frac{A_h \rho c_p V_h T_h - \lambda_f \frac{dT_h}{dx} A_h}{H1}$$

$$= \rho c V_h \left( T_h + \frac{dT_h}{dx} dx \right) A_h - \left\{ \lambda_f \frac{dT_h}{dx} + \frac{d}{dx} \left( \lambda_f \frac{dT_h}{dx} \right) dx \right\} A_h$$

$$\frac{H2}{+ \kappa_h (T_h - T_\infty) p_h dx + h_{eq} (T_h - T_c) dA}$$

$$\frac{H3}{4}$$

$$(7)$$

Returning region

$$\frac{-A_c \rho c_p V_c T_c - \lambda_f \frac{dT_c}{dx} A_c}{C1}$$

$$= -\rho c V_c \left( T_c + \frac{dT_c}{dx} dx \right) A_c - \left\{ \lambda_f \frac{dT_c}{dx} + \frac{d}{dx} \left( \lambda_f \frac{dT_c}{dx} \right) dx \right\} A_c$$

$$\frac{C2}{+ h_{eq} (T_h - T_c) dA}$$

$$4$$

$$(8)$$

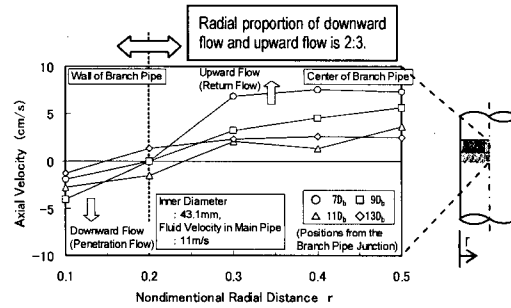


**Fig.11 Axial Velocities of Cavity Flow**

## 5.3 Calculation of Natural Convection

### Phenomenon

In this method, natural convection region is divided into two region as is shown in figure 12, i.e. hot layer and cold layer, and the fundamental equations 9 and 10 are formulated based on the heat balance in the infinitesimal section as following.

- (1) Inflow and outflow of heat due to fluid motion and heat conduction
- (2) Heat removal from natural convection region to atmosphere
- (3) Heat transfer from incoming region to returning one.

The ratio of the hot layer and cold layer is 3:1 in the cross-section and that are obtained from experimental results.

Hot layer

$$\frac{A_h \rho c_p U_h T_h - \lambda_f \frac{dT_h}{dx} A_h}{H1}$$

$$= \rho c U_h \left( T_h + \frac{dT_h}{dx} dx \right) A_h - \left\{ \lambda_f \frac{dT_h}{dx} + \frac{d}{dx} \left( \lambda_f \frac{dT_h}{dx} \right) dx \right\} A_h$$

$$\frac{H2}{+ \kappa_h (T_h - T_\infty) p_h dx + h_{eq} (T_h - T_c) dA}$$

$$\frac{H3}{4}$$

$$(9)$$

Cold layer

$$\frac{A_c \rho_c \rho_p U_c T_c - \lambda_r \frac{dT_c}{dx} A_c}{C1} = \rho_c \rho_p U_c \left( T_c + \frac{dT_c}{dx} dx \right) A_c - \left\{ \lambda_r \frac{dT_c}{dx} + \frac{d}{dx} \left( \lambda_r \frac{dT_c}{dx} \right) dx \right\} A_c \quad C2$$

$$\frac{+ \kappa_c (T_c - T_{eq}) \rho_c dx - h_{eq} (T_h - T_c) dA}{C3 \quad 4} \quad (10)$$

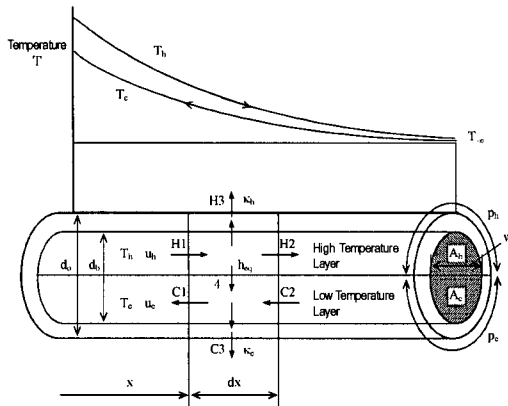


Fig.12 Outline of Natural Convection Model

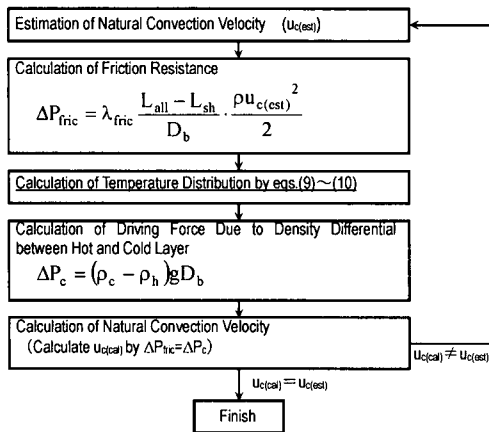


Fig.13 Flow Diagram of Temperature Distribution Calculation in Natural Convection Region

#### 5.4 Ratio of Heat Input and Heat Removal $\chi$

The correlation of the ratio of heat input and heat removal  $\chi$  is the function of the energy of cavity flow and heat removal from natural convection region as

shown in figure 14, and that is expressed by the following expression.

$$Q^* = \frac{Q_{outH}}{Cp \cdot \rho \cdot D_b^2 \cdot u \cdot T} \quad (11)$$

where, Cp: specific heat of fluid,  $D_b$ : inner diameter of branch pipe, u: vortex velocity in tangential direction of branch pipe

Applying the equation 11 to the function  $\chi$  having best fitting to the experimental results, following equation is obtained

$$\chi = 1 - \exp\left(-6000 \cdot \frac{Q_{outH}}{Cp \cdot \rho \cdot D_b^2 \cdot u \cdot T}\right) \quad (12)$$

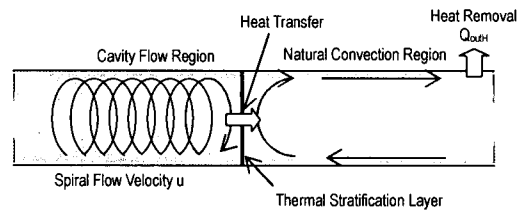


Fig.14 Heat Transfer from Cavity Flow Region to Natural Convection Region at Thermal Stratification Layer

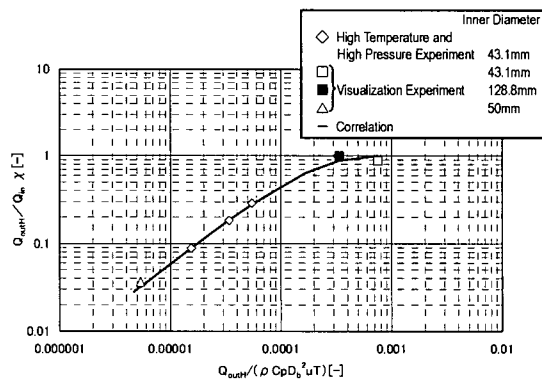


Fig.15 Correlation of  $\chi$

#### 6. VERIFICATION

The evaluation method for  $L_{sh}$  is verified with the visualization experiments and the high temperature and high pressure experiments.

The verification results are shown in table 1. The predictive accuracy of the evaluation method for  $L_{sh}$  is about  $\pm 20\%$ . Figure 16 shows the comparison of the

experiment and the analysis for the temperature distribution over the branch pipe. It is confirmed from those results that the evaluation method of  $L_{sh}$  can estimate penetration length of cavity flow well.

## 7. CONCLUSIONS

The visualization and high temperature and high pressure experiment were carried out to clarify the characteristics of cavity flow which penetrated into a one-side-closed branch pipe connecting to a main pipe with constant flow rate. Based on those experimental results, the evaluation method for  $L_{sh}$ , penetration length of cavity flow in a vertical branch pipe with a horizontal branch pipe connected by an elbow, is developed. The predictive accuracy of the evaluation method for  $L_{sh}$  is  $\pm 20\%$ .

## ACKNOWLEDGEMENT

This research is a utility-vendor joint research project on thermal stratification layer due to cavity flow in a branch pipe. These results have been reviewed by a working group in the JSME to draft a code concerning high-cycle thermal fatigue of piping systems. The authors would like to take this opportunity to express their sincere gratitude to all working group members for their important advice and support.

## REFERENCES

- (1) Nakamori, N., et al., NURETH6, Vol.1, pp415-424, (1993).
- (2) Tanimoto, K., et al., ASME/JSME Proc. 10<sup>th</sup> Int. Conf. Nuclear Engineering, No.23340, (2002).
- (3) Shiraishi, T., et al., SVS2000 (FVSI, Sapporo, 2000).
- (4) Shiraishi, T., Tanimoto, K. and Suzuki, S., Symposium on Flow Modeling and Turbulence Measurement (FMTM2001), Nov.4-6, (2001).
- (5) Tanimoto, K., et al., 2002 Annual Meeting of the JSME (2002-9), F11-(6).
- (6) Tanimoto, K., et al., The 3<sup>rd</sup> Korea-Japan Symposium on Thermal-Hydraulics and Safety (NTHAS3) (2002), NTHAS3-054.
- (7) Tanimoto, K., et al., 2002 Annual Meeting of the Atomic Energy Society of Japan, L6, (in Japanese).

**Table 1 Verification Results of the Evaluation Method of  $L_{sh}$**

Experimental Condition			Penetration Length of Cavity Flow			Inner Diameter of Branch Pipe
Experiment	Branch Pipe Condition	Main Pipe Condition	Calculation (C)	Experiment (E)	C/E	
Visualization Experiment	Acrylic Resin Pipe	5m/s	13.2	13	1.02	50mm
		7m/s	15.4	15	1.05	
		11m/s	17.3	15	1.15	43.1mm
			11.0	13	0.85	
			15m/s	15.2	19	
High Temperature and High Pressure Experiment	with Insulation	320°C	16.7	18	0.93	43.1mm
			14.6	17	0.86	
			14.0	15	0.93	

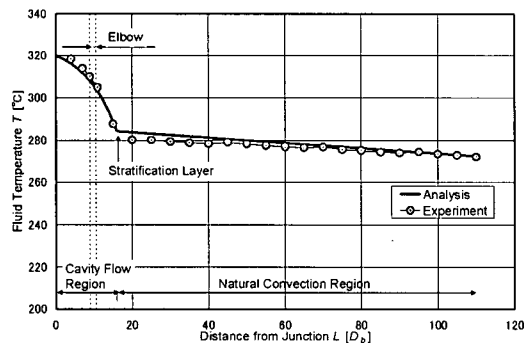


**Fig. 16 Verification Results for High Temperature and High Pressure Experiment.**  
 (50Asch160 (Inner Diameter :43.1mm),  
 Length of Branch Pipe : Vertical Pipe  $9D_b$ ,  
 Horizontal Pipe  $100D_b$ )